
Can Differentiable Decision Trees Learn Interpretable Reward Functions?

Akansha Kalra, Daniel S. Brown
Kahlert School of Computing
University of Utah
akanshak@cs.utah.edu, dsbrown@cs.utah.edu

Abstract

There is an increasing interest in learning reward functions that model human intent and human preferences. However, many frameworks use blackbox learning methods that, while expressive, are difficult to interpret. We propose and evaluate a novel approach for learning expressive and interpretable reward functions from preferences using Differentiable Decision Trees (DDTs). Our experiments across several domains, including Cartpole, Visual Gridworld environments and Atari games, provide evidence that the tree structure of our learned reward function is useful in determining the extent to which the reward function is aligned with human preferences. We experimentally demonstrate that using reward DDTs results in competitive performance when compared with larger capacity deep neural network reward functions. We also observe that the choice between soft and hard (argmax) output of reward DDT reveals a tension between wanting highly shaped rewards to ensure good RL performance, while also wanting simple, non-shaped rewards to afford interpretability.

1 Introduction

Deep Reinforcement Learning (RL) methods in recent years have made significant strides in learning to play games [45, 18, 14], successfully completing tasks in simulated environments [31, 66, 39, 33], and in solving real robotics tasks [28, 32, 63, 1]. While the reward function is central to RL algorithms, it is often difficult to manually specify [47, 38], motivating learning reward functions from human input [52, 18, 15, 10, 7]. In this paper, we focus on the problem of learning interpretable reward functions.

Most modern reward learning methods use deep neural networks [21, 18, 32, 33]. However, despite the growing interest in explaining deep neural networks [26, 65, 30, 50], deep neural networks remain extremely difficult to interpret. This inherently poses the question of how we can trust what our neural network has learned if we can not comprehend and infer the representations it has learned?

In the context of reward learning, it is especially critical that we can interpret the learned objective—if we can not understand the objective that a robot or AI system has learned, then it is difficult to know if the AI’s behavior will be aligned with human preferences and intent [51, 41, 17]. This is particularly significant in tasks where human safety is on the line, for example in autonomous navigation systems and assistive robots.

Thus, we are faced with a problem. We want highly accurate and expressive models, but we also want to be able to explain and interpret the reward functions that an AI system has learned. A natural step towards both of these goals is to combine the expressiveness of neural networks with an architecture choice that is easy for a human to interpret, such as a decision tree. Similar to our approach, Bewley et al. [7, 6] learn a tree-structured reward function given preferences over trajectories. However, their approach has several limitations which we seek to address: (1) prior work requires hand-specification

of feature space for learning the reward, (2) is not end-to-end differentiable, and (3) cannot be scaled easily to high dimensional inputs such as images.

To tackle the the aforementioned problems, we propose a novel reward learning approach that uses an end-to-end differentiable decision tree model for learning interpretable reward functions from pairwise preferences. We evaluate our approach on three different domains: Cartpole [13], Visual MNIST Gridworld environments, and two Atari games from the Arcade Learning Environment [5]. Our results demonstrate the ability to learn expressive and interpretable reward functions from both low- and high-dimensional state inputs.

Learning a reward model as a differentiable decision tree (DDT) has the advantage that the tree structure explicitly breaks the reward prediction for a state into a finite number of routing decisions within the tree. This provides the potential to understand how the reward predictions are being made. Our results demonstrate that we can leverage the interpretability of the learned reward DDT to identify spurious correlations and misalignment in the learned reward model. Our framework generates global explanations for all inputs across both low- and medium-dimensional environments such as Cartpole and visual MNIST gridworld. For high-dimensional visual state space, such as Atari, we propose a novel form of hybrid explanation that approximates global explanations by leveraging aggregations of local explanations using individual input states.

This paper makes the following contributions:

1. We introduce a reward learning framework that employs differentiable decision trees to learn human intent using trajectory preference labels without necessitating any hand-crafting of the input feature space.
2. We propose hybrid explanations that our framework generates by approximation of global explanations by leveraging aggregations of local explanations using individual input states.
3. We study the ability of Differential Decision Trees(DDTs) to learn interpretable rewards across several domains including complex visual-control tasks and find that our Reward DDTs can learn an interpretable reward function with RL performance comparable to that of a black-box neural network.

2 Related Work

Preference Learning Learning from human pairwise preferences over trajectories is a common approach to learning reward functions and corresponding RL policies [62, 18]. Preference learning is a general technique that is useful across multiple modalities of human input: prior work has shown that other forms of feedback, such as demonstrations [16], e-stops [24], and corrections [43], can all be represented in terms of preferences. Thus, our approach is applicable, even when pairwise preference labels are not explicitly available. Prior work on learning reward functions from preference labels typically either assumes access to a set of hand-designed reward features [53, 8, 24] or uses deep convolutional or fully connected networks for reward learning [18, 15, 39, 33, 56, 42]. By contrast, we study the extent to which we can learn expressive, but also interpretable reward functions from preferences via differentiable decision trees.

Explaining and Interpreting Reward Functions In the past few years, various attempts have been made to understand learned reward functions whether it’s by comparing the learned reward function to ground truth reward using a pseudometric [27], by using saliency maps and counterfactuals [15, 44], by leveraging human teaching strategies [40, 11], or by using human-centric evaluation methods for reward explanation [54]. Recent work has shown that reward functions learned from human preferences via deep neural networks often suffer from spurious correlations and reward misidentification [?]. In this work we seek to investigate to what extent differentiable decision trees enable interpretable reward functions and whether these learned reward functions enable the identification of reward misidentification.

Differentiable Decision Trees Differential Decision Trees (DDTs), also referred to as Soft Decision Trees, seek to combine the flexibility of neural networks with the interpretable structure of decision trees. Differentiable decision trees have been previously applied to supervised learning tasks [23, 59, 29] and unsupervised tasks [64]. Recent work has investigated using DDTs for reinforcement

learning tasks [57, 19, 58, 20, 48], but focus on *policy learning* using DDTs. Compared to prior work, the primary objective of our work is to *learn interpretable reward functions* using DDTs. Policy explanations are very important, but they only show what triggers an agent to take an action, but not reason for taking the action. By understanding agent’s reward, we gain insight into the agent’s value alignment which can transfer across different embodiments and dynamics, unlike policies. Furthermore, prior work using DDTs for policy learning only considers low-dimensional, non-visual inputs [57, 19]. By contrast, we study DDTs applied to high-dimensional image observations.

Decision Trees for Reward Learning There has been very little prior work on using decision trees for reward learning. Bewley et al. [7] formulate a tree-based reward learning method that requires a complex, non-differentiable, multi-stage optimization procedure. By contrast, our approach is end-to-end differentiable and trainable using a simple cross entropy loss. Bewley et al. [7] only consider low-dimensional inputs where internal nodes in the tree have the form $(s, a)_d \geq c$ for each dimension d of the state-action space and threshold c . This approach divides the state-action space into axis aligned hyperrectangles, which works for lower-dimensional spaces, but does not scale to higher-dimensional state and action spaces. More recent work by Bewley et al. [6] uses a differentiable loss function but is not end-to-end differentiable as it requires the reward tree to regrow at each update. Furthermore, their approach requires hand crafting input features per decision node in the decision tree which makes it intractable to scale to the types of visual inputs we consider.

3 Reward Learning using Differentiable Decision Trees

Classical decision trees are easy to tune and are often quite interpretable [37, 46]; however, they require feature engineering which can result in lower performance and loss of generalization when compared with other machine learning approaches [23, 29]. In this section we discuss our proposed approach for learning interpretable but expressive reward functions via differentiable decision trees (DDTs). DDTs are well suited for this task since they are more expressive than a classical decision tree, exhibit better generalization capabilities, and retain interpretability [23, 59, 29].

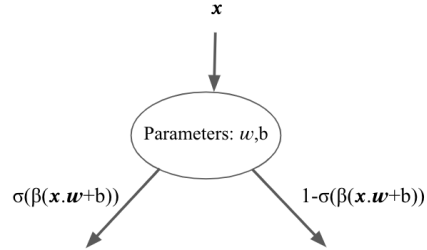


Figure 1: Routing Probability of an internal node in a differentiable decision tree (DDT).

3.1 Internal Nodes

Classical decision trees consist of nodes that deterministically route inputs. Because we want our reward function tree to be easily trained using backpropagation, we need to define a soft routing function that is differentiable and retains the expressiveness of a neural network by learning the routing function for each non-leaf node.

An internal node in the DDT consists of a sequence of one or more transformations applied to the input to the DDT, in order to obtain the routing probability for traversing the tree after the given node. We describe two variants of an internal node below:

Simple Internal Node First proposed by Frosst and Hinton [23], a simple internal routing node, i , has a linear layer with learnable parameters \mathbf{w}_i and a bias term b upon which sigmoid activation function, σ , is applied to derive the routing probability given an input \mathbf{x} . Thus, the probability at node i of routing to the left branch is defined as

$$p_i(\mathbf{x}) = \sigma(\beta(\mathbf{x} \cdot \mathbf{w}_i + b)) \tag{1}$$

An inverse temperature, β , is included in the equation above for controlling the degree of soft decisions. In this way, each internal node depends directly on the input (Figure 1). The differentiable decision tree learns a hierarchy of decision boundaries that determine the routing probabilities for each input.

Sophisticated Internal Node For higher-dimensional inputs (e.g. the Atari games we study), we propose an alternative internal node architecture. The input \mathbf{x} is first transformed by a convolutional

layer with Leaky ReLU as the non-linearity followed by a fully connected linear layer, as before. The probability of going to the leftmost branch at an internal node i is defined as

$$p_i(\mathbf{x}) = \sigma((\text{LeakyReLU}(\text{Conv2d}(\mathbf{x}))) \cdot \mathbf{w}_i + b) \quad (2)$$

In Appendix C.3, we examine the effect of the choice of internal node architecture on the interpretability of the reward DDT.

3.2 Leaf Nodes

Owing to soft routing at internal nodes, each leaf node in the tree has a routing probability associated with it, thus we can think of the DDT as a hierarchical mixture of experts [35]. Following prior work that uses DDTs for classification problems [23], a leaf node l is parameterized by ϕ^l , a vector of dimension $1 \times c$ where c is number of output classes. The learned vector ϕ^l defines a softmax distribution over a discrete number of reward outputs. The probability distribution over classes, \mathbf{Q}^l , is defined as

$$\mathbf{Q}_c^l = \frac{e^{\phi_c^l}}{\sum_{c'} \phi_{c'}^l} \quad (3)$$

We propose and study two ways to obtain rewards at the leaves of a reward DDT.

Multi-Class Reward Leaf This straightforward approach follows directly from multi-class classification and assumes that the user can specify classes of possible reward values suitable for the given task. The user provides a discrete vector of possible reward values $\mathbf{R} = (r_0, r_1, \dots, r_{c-1})$, where c denotes the number of classes for the DDT, where each class index i is assigned reward value r_i . The learnable parameters ϕ^l at leaf l form the logit values of a classification problem over the possible reward values in \mathbf{R} .

Min-Max Reward Interpolation Leaf As an alternative to the classification approach, we can model the reward of a DDT as a *regression problem*. Instead of requiring the user to specify a finite set of possible reward values that the tree can output, we only require the user to specify a minimum and maximum range of possible reward values. Thus, the reward vector is of the form $\mathbf{R} = (R_{\min}, R_{\max})$, where R_{\min} and R_{\max} correspond to minimum and maximum of the user-defined range of rewards. Given this parameterization, we can view the reward output of a DDT as a convex combination of R_{\min} and R_{\max} based on the learned parameters ϕ^l .

3.3 Training Differentiable Decision Trees for Reward Learning using Human Preferences

We now describe how to use a DDT for reward learning. We want our reward DDT to be end-to-end differentiable when learning a reward function from preference labels. We accomplish this during training by having the tree output a soft reward prediction as follows. First, the tree of depth $d \geq 1$ is built by $\sum_{k=0}^{d-1} 2^k$ internal nodes and 2^d leaves. Given an input \mathbf{x} , the path probability from root node to a leaf l is denoted by $P^\ell(\mathbf{x})$ and the soft reward prediction of the tree is given by the sum over all leaves of the path probability of reaching that leaf $P^\ell(\mathbf{x})$, multiplied with the soft reward at the leaf:

$$r_\theta(\mathbf{x}) = \sum_{\ell} P^\ell(\mathbf{x})(\mathbf{Q}^\ell \cdot \mathbf{R}) \quad (4)$$

To train our reward function DDT, we propose to leverage pairwise preference labels over trajectories. This is a popular method for training reward functions because of the ease of obtaining preferences rather than actual demonstrations [61, 18] and because preference-based reward learning removes the need to repeatedly solve or (partially solve) the computationally-expensive forward RL problem to obtain a reward estimate [3, 15].

Given preferences over trajectories of the form $\tau_i \prec \tau_j$, where $\tau = (s_1, s_2, \dots, s_T)$, we can train our entire differentiable decision tree via the following cross entropy loss resulting from the Bradley Terry model of preferences [12]:

$$\mathcal{L}(\theta) = - \sum_{\tau_i \prec \tau_j} \log \frac{\exp \sum_{s \in \tau_j} r_\theta(s)}{\exp \sum_{s \in \tau_i} r_\theta(s) + \exp \sum_{s \in \tau_j} r_\theta(s)} \quad (5)$$

Table 1: Evaluating RL on Learned Reward Function in CartPole. We report the Inter-Quartile Mean (IQM) across 3 seeds where each seed’s performance is averaged over 100 rollouts. We find that DDTs with argmax outputs outperform soft rewards at test time and that both significantly outperform RL performance of a non-interpretable fully connected 2-layer reward network baseline. CRL denotes a tree with Class Reward Leaf nodes.

	DDT		Baseline
	CRL Soft	CRL Argmax	Neural Network
IQM	68.7	161.8	9.5

For DDTs with sophisticated nodes, we also analyze a modified version of Equation (5) with an added penalty term that regularizes the network to ensure that, on average across many inputs, each internal node routes left and right equally often (see Appendix A for details).

3.4 Using a Trained Reward DDT for Reward Prediction

Given a trained reward DDT, there remains the question of how to use it for reward prediction at test time (e.g., when using the reward DDT for reinforcement learning). One option is to use the soft reward (averaged across all leaf nodes weighted by routing probability); however, this loses interpretability since we cannot trace the predicted reward to a small number of discrete decisions. To enable interpretable reward predictions we can output a single reward prediction as follows. First, given an input \mathbf{x} , we find the leaf node with maximum routing probability

$$l^* = \arg \max_{l \in L} P^l(\mathbf{x}) \tag{6}$$

where L denotes set of all leaf nodes in the DDT. And then based on leaf formulation of the DDT, the test-time output of a reward DDT with Multi-Class Reward Leaf nodes is given as

$$r_{max}(\mathbf{x}) = r_i, \text{ for } i = \arg \max_i \mathbf{Q}_i^{\ell^*} \tag{7}$$

while the test-time output of a reward DDT with Min-Max Reward Interpolation Leaf nodes is

$$r_{max}(\mathbf{x}) = \mathbf{Q}^{\ell^*} \cdot (R_{\min}, R_{\max}). \tag{8}$$

4 Experiments and Results

We evaluate the performance and interpretability of reward DDTs on three different environments: classic CartPole control problem, a novel set of MNIST Gridworld environments, and finally on games from the Atari 2600 game suite [4]. Note that we refer to *multi Class Reward Leaf tree* as **CRL** and *min-max reward Interpolated Leaf tree* as **IL**.

4.1 CartPole

The CartPole environment comprises a cart with a pole attached to it, sliding on a friction-less track. The objective is to balance the pole on the cart for as long as possible while the cart moves to left and right along the track without letting the pole fall beyond $\pm 12^\circ$ from the upright position and without letting the cart move beyond ± 2.4 units along the track. Thus, the ground-truth reward is a function of only cart position and pole angle. We assume no access to ground truth reward and we use our DDT framework to learn the ground-truth reward from pairwise preference labels.

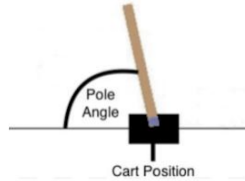


Figure 2: The CartPole environment consisting of pole attached to a cart, that moves along the track.

Setup To train a reward function DDT, we generate a wide variety of trajectories by running a random policy in the environment for 200 steps for each trajectory. We assume no access to any kind of terminal or done flag (since this would leak significant information about the true reward [22]). Thus, we ignore the done flag in the cartpole environment and keep accumulating states in the

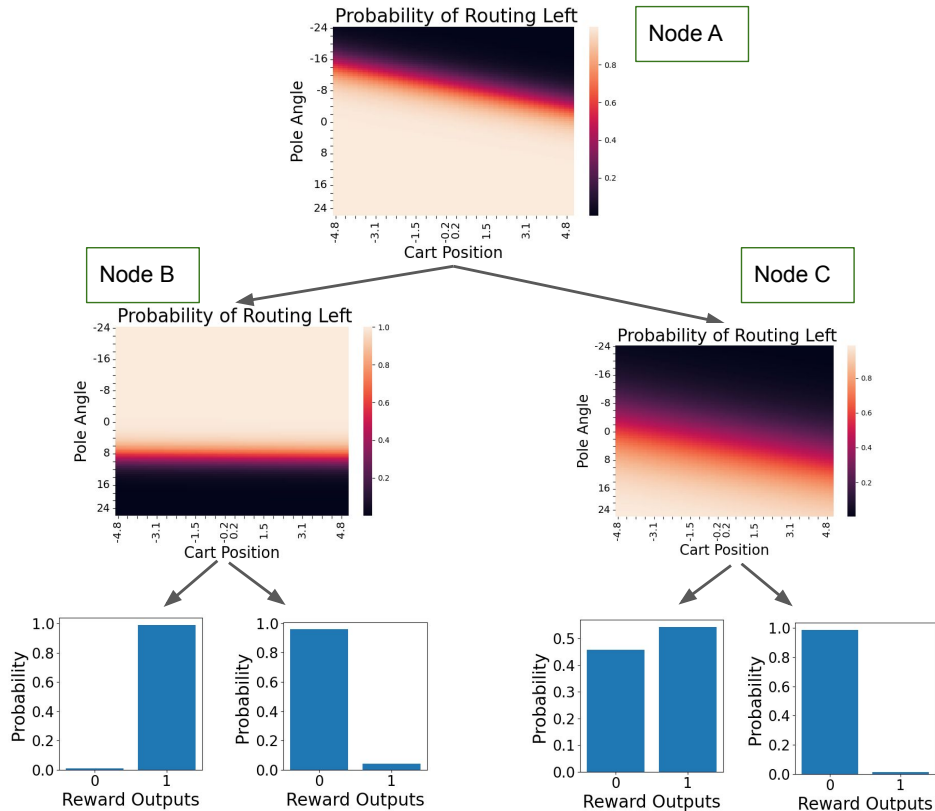


Figure 3: **Cartpole Reward DDT of Depth 2.** The heatmap for each internal node depicts the learned routing probability. Bar graphs on leaves depict the probability distribution of the reward outputs. The tree learns that small magnitude pole angles are good and should be routed to a +1 reward but there is no learned decision boundary that clearly captures the preference that cart position stay within the range $[-2.4, 2.4]$ showing that learned reward is mis-aligned.

trajectory for 200 timesteps, even if the pole falls over. We design a synthetic preference labeler that returns pairwise preferences based on the true (but unobserved) reward of +1 only if the cart position $x \in [-2.4, 2.4]$ and the pole angle $\theta \in [-12^\circ, +12^\circ]$ and 0 otherwise. Pairwise preferences are assigned based on the cumulative rewards for each trajectory. Given pairwise preference labels over these suboptimal trajectories, we train a reward DDT of depth 2: the tree has 3 internal nodes and 4 leaf nodes (we experimented with larger depth and did not see any improvements in performance). We use multi-class reward leaf nodes with two classes: $\mathbf{R} = (0.0, 1.0)$. This is because the true reward is binary and we wish to compare the results of the reward DDT to the ground truth reward. We use a learning rate and weight decay both equal to 0.001 and the Adam optimizer.

It is important to note that even though the ground truth preferences are based on both cart position and pole angle, the pole usually falls past the desirable range long before the cart leaves the desirable range. Thus, our dataset is biased and we hope to be able to pickup on this bias, and the corresponding misaligned reward function by inspecting the learned reward DDT.

To evaluate the RL performance of the learned reward function by the DDT, we train a PPO [55] agent on the learned reward function to obtain the final policy and then evaluate this learned policy on the ground-truth reward function. We provide Inter-Quartile Mean (IQM) [2] across 3 seeds where each seed’s performance is averaged over 100 rollouts. We also compute the ground-truth performance of a PPO policy trained on using a neural network reward function. The neural network reward function is trained using the same dataset of pairwise preferences and is comprised of 2 fully connected layers with Leaky ReLU as non-linearity between the layers and the output from the last fully connected layer goes through a sigmoid activation for the final reward from the neural network.

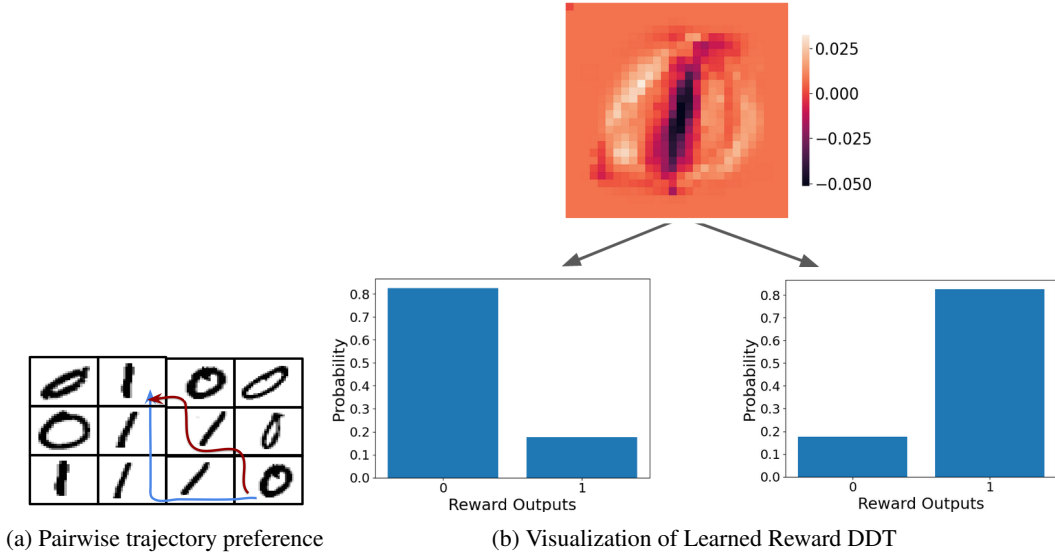


Figure 4: **MNIST (0/1) Gridworld.** (a) A pair of trajectories that both reach the same state. The blue trajectory (which visits more 1’s) is preferred over the red trajectory. (b) DDT of depth 1 with heatmap at the root node illustrating the difference in routing probability of each pixel when it is on versus off. The dark pixels in the center of heatmap represent an approximate shape of digit 1 and are routed to right as the dark colors in heatmap mean that those pixels are turned off. Similarly the pixels with slight white light represent an approximate shape of digit 0 and are routed to left as the lightest colors in heatmap mean that those pixels are turned on. The bar graphs depict the probability distribution of reward outputs at each leaf node.

Results Figure 3 shows the learned reward DDT. Because the input space to the reward function is 2-dimensional (cart position and pole angle) we visualize the heatmap of routing probability at each internal node (as a function of cart position and pole angle) along with plots of the leaf distribution over output classes. From the DDT it is clear that most of the routing decisions are made based on the pole angle, rather than the cart position. A nice feature of the reward DDT is that we can easily visually interpret the learned reward just by looking at the tree (without requiring privileged information about the true reward function). From Figure 3 we see that while the tree learns that small magnitude pole angles are good and should be routed to a +1 reward, there is no learned decision boundary that clearly captures the preference that cart position stay within the range $[-2.4, 2.4]$.

The results in Table 1 show that a simple reward DDT outperforms a neural network made up of fully-connected layers, irrespective of whether the policy is learned using soft rewards or using the maximum probability path across the learned reward DDT.

4.2 MNIST GridWorld

Next, we use our reward DDT framework for solving MDPs with visual inputs. We propose two novel gridworld environments where each state is associated with an MNIST digit and the value of the digit determines the true reward at that state.

4.2.1 MNIST (0/1) Gridworld

Setup Here the MDP is a 5x5 gridworld where each state s in the MDP corresponds to a 28×28 greyscale images of the digits 0 or 1. The action space a contains 4 main actions: go left, go right, move up, move down. The transition function is stochastic and moves the agent in the direction chosen with an 80% probability as long as the action does not take it off of the grid. Actions that would result in leaving the grid result in a self transition. The true (unobserved) reward function is the value of the MNIST digit. Thus, landing on an image of the digit 1 has a true reward of 1 and landing on the digit 0 has a true reward of 0. Note, however, that these rewards are never observed

and must instead be inferred from pairwise preferences over trajectories consisting of multiple 1’s and 0’s as shown in Figure 4a.

We train a DDT using pairwise preferences over randomly sampled trajectories over randomly generated MDPs, where each trajectory is a sequence of states and each 28×28 greyscale input image is treated as an individual state. Given two such sequences of trajectories of equal length, the preference label is assigned based on comparison between the sum of ground truth labels of each input image comprising the respective trajectories.

To test whether we can learn an interpretable reward function, we modeled the reward as a DDT of depth 1 with one simple internal node as the root node and 2 multi-class reward leaf nodes. The DDT is trained on pairs of preference demonstrations over trajectories (see Figure 4a for an example pairwise trajectory comparison). We set the reward vector $\mathbf{R} = (0.0, 1.0)$ where $R_{\min} = 0$ and $R_{\max} = 1$ and for training the DDT, we use a learning rate of 0.001, weight decay of 0.05, and the Adam optimizer [36].

Results After training the reward DDT, we construct an activation heatmap for each internal node by starting with a blank image and iteratively toggling on and off each pixel and computing the difference in routing probabilities at the root node. The resulting heatmap in Figure 4b demonstrates the fact that DDT learns to branch based on visually interpretable features that correspond to a 0 (routes to left leaf node) and 1 (routes to right leaf node).

We evaluate the RL performance of the policy extracted from the learned reward function against the optimal policy under the ground truth reward, and compare it to performance of a random policy as well as to policy learnt by a neural network comprising of 2 convolutional layers with kernel size 7 and 5 respectively and stride 1 with LeakyRelu as the non-linearities followed by 2 fully connected layers trained using pairwise human preferences. We summarize the results of our evaluation as the average of ratio between given policy to the optimal ground truth policy across 100 different MDPs with states as digits 0 or 1. The RL performance using the Soft Reward from Class Reward Leaf DDT on MNIST 0-1 environment is shown in Table 2 comparable to a deep neural network reward function trained on pairwise preferences. We observe that taking the maximum probability path across the learned reward tree results in a small loss of performance relative to when we take soft reward from the learned DDT but still is significantly better than random policy.

4.2.2 MNIST (0-3) Gridworld

Setup We increased the complexity of the reward function such that the states in the MDP correspond to MNIST digits 0, 1, 2, and 3, while the action space and transition function remain exactly the same as before. The unobserved true reward function r (used to provide preferences over trajectories) provides a reward of 0.0, 1.0, 2.0, 3.0 upon reaching a state with an image of the digit 0, 1, 2, and 3, respectively.

We trained two different types of reward DDTs. First, we modeled the reward using a DDT of depth 2 with 3 simple internal nodes and 4 multi-class reward leaves with $\mathbf{R} = (0, 1, 2, 3)$. Second, we modeled the reward using the same internal structure but with min-max reward interpolation leaves using $R_{\min} = 0$ and $R_{\max} = 3$. For both tree structures, we trained using a learning rate of 0.001 and weight decay 0.005 and the Adam optimizer. We evaluate the RL performance of the policy extracted from the learned reward function against the optimal policy under the ground truth reward, and compare it to performance of a random policy as well as the performance of RL when using a neural network with the same architecture as Section 4.2.1 trained using pairwise human preferences.

Results In Appendix C we visualize and compare the reward DDTs learned using multi-class leaf nodes and min-max interpolation leaf nodes. We find that when using multi-class leaf nodes the leaf nodes fail to specialize and the argmax output of the leaf nodes is either 0 or 3. We investigated several regularization methods (see Appendix C), but found that none of these helped. Our conclusion is that using the min-max reward interpolation nodes is best when dealing with learning complicated reward functions where we wish to output more than two possible rewards. It is also simpler, since it only requires the human to specify a range of desired reward values, $[R_{\min}, R_{\max}]$. Thus, we focus on our analysis of the interpretability of the min-max reward interpolation DDT.

Figure 5 shows activation heatmaps of the node probability distribution at each of the internal nodes. These activation heatmaps are not simply combinations of digits like Figure 4, but rather isolate pixel

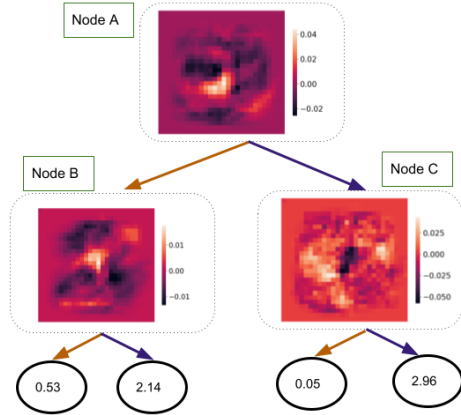


Figure 5: **Visualization of MNSIT (0-3) Reward DDT trained on longer trajectories.** The activation maps provide interpretability and show that images of 1s are routed left to node B and then left to the leaf node that outputs 0.53. Images of 0s are routed from Node A to node C then to the 0.05 leaf node. Images of 2s are routed from A to B then to 2.14. Images of 3s are routed from A to C then to 2.96.

Table 2: RL Performance as the percentage of given policy to the optimal ground truth policy across 100 different MDPs in 3 Gridworld environments. We find that trees with Interpolated Leaf nodes (IL) perform as well as a neural network reward in both gridworld environments, while using Class Reward Leaf nodes (CRL) results in lower performance, but still significantly outperforms a random policy (Random). This verifies that our simple framework can learn interpretable reward without losing the expressiveness of a neural network under RL evaluation.

	DDT				Baseline	
	CRL Soft	CRL Argmax	IL Soft	IL Argmax	NNet	Random
MNIST 0-1	92.37%	82.27%	99.98	100%	98.2%	7.38%
MNIST 0-3	71.66%	71.66%	98.99%	97.77%	99.53%	7.56%
MNIST 0-9	62.15%	62.15%	97.32%	92.87%	97.74%	7.93%

features that are maximally discriminative. However, they still provide a strong understanding of what the network has learned and how it predicts rewards. These heatmaps show that DDT learns to route based on visual representations of each digit: Node B routes left for vertical pixels in the center from vertical stroke of digit 1 and sends 1’s left while using upper and lower curves of digit 2 to route 2’s right (note the black shadow that looks like a 2). To discriminate between a digit 0 and 3, node C discriminates based on middle cusp of 3 and left curve of the 0. Finally, node A learns that what best distinguishes 1s and 2s from 0s and 3s is presence of central lower pixels—the highest activation for node A is intersection of the 1 and 2 which falls between middle and lower cusps of 3 and inside digit 0. Note that the tree uses min-max reward interpolation between $R_{min} = 0$ and $R_{max} = 3$. There are no explicit reward labels, just pairwise preferences over trajectories. Despite the lack of fine-grained feedback, the DDT learns a close approximation to the actual state rewards and the learned rules in the DDT are interpretable.

We summarize the results of our evaluation as average of ratio between given policy to the optimal ground truth policy across 100 different MDPs consisting of digits 0,1,2 and 3. Table 2 shows that the RL performance of the interpolated leaf (IL) reward DDT far exceeds the performance of the class reward leaf (CRL) DDT, both when the optimal policy is trained using soft reward outputs and when optimal policy is trained using the output of the maximum probability path in the tree. The RL performance of the IL reward DDT using soft reward is comparable to performance of a deep neural network reward function and is higher than that of a policy trained using argmax reward outputs.

In Appendix C, we compare the reward DDT in Figure 5 learned from pairwise preferences with a DDT trained with explicit reward labels and a classification loss and find no significant degradation in interpretability from using pairwise preferences. This is encouraging since requiring someone to hand label each individual state with reward values is much more cumbersome than requiring binary preference labels over trajectories.

4.2.3 MNIST (0-9) Gridworld

Setup To assess the scalability of our framework for long-term planning tasks, we test reward DDTs on 10x10 gridworlds that now correspond to MNIST digits 0, 1, 2, 3, 4, 5, 6, 7, 8 and 9. As before, the unobserved true reward function r (used to provide preferences over trajectories) provides a reward equal to the value of the digit.

We train 2 reward DDTs of depth 4 with simple internal nodes where the first tree has the multi-class reward leaves with $\mathbf{R} = (0, 1, 2, 3, 4, 5, 6, 7, 8, 9)$, while the second tree has min-max reward interpolated leaves with reward vector $\mathbf{R} = (0, 9)$. We report the results of our RL evaluation in row 3 of Table 2 as average of ratio between given policy to the optimal ground truth policy across 100 different MDPs. We evaluate the policy extracted from the learned reward function against the optimal policy under the ground truth reward, and compare it to performance of a random policy as well as to policy learned by a neural network with the same architecture described in Section 4.2.1.

Results Row 3 of Table 2 shows IL’s soft reward performs comparable to black-box convnet reward with IL’s argmax performance is lower by a very small margin but CRL’s both softmax and argmax performance is hugely degraded while still being better than the random policy. This provides evidence that our framework maintains high performance for much longer horizon and more difficult tasks. We analyzed learned DDT and find it still retains explainability despite increase in depth, while still performing comparably to a black-box reward learning approach.

4.3 Atari

To stress test the efficacy of learning rewards via DDTs, we evaluate learning a reward DDT on the Beam Rider and Breakout Atari games. Learning rewards for these games is quite challenging and requires learning a reward from visual inputs consisting of stacks of four frames from the video games.

Setup To generate pairwise preference demonstrations for training the DDT, we first generate the demonstrations using Proximal Policy Optimization (PPO) [55] policies checkpointed every 50 training update for each game. Using the demonstrations we construct pairwise preferences over randomly sampled trajectory snippets using the same procedure proposed by Brown et al. [15] who learned reward functions using deep convolutional neural networks for these games. We seek to test whether a reward DDT can match the RL performance of the T-REX deep neural network trained by Brown et al. [15], while being interpretable.

Because of the complexity of the task, we use sophisticated internal nodes for routing. These internal nodes are now constructed to include a single convolutional layer with kernel of size 7×7 with a stride of 2 and LeakyRelu as the non-linearity before the fully connected linear layer for producing the routing probability inside a tree. The input for a simple DDT for all Atari games, is very high-dimensional visual input with 4 frames of size 84×84 stacked together. The input to DDT here is a 5-dimensional tensor of size $B \times 2 \times S \times 84 \times 84 \times 4$ where B represents batch size of pairwise preference demonstrations while 2 is represents of number of demonstrations in a pairwise preference and S represents number of states in a single trajectory. For all games, we use sophisticated internal nodes for training the reward DDT of depth 2 and used min-max reward interpolation leaf nodes with $R_{\min} = 0$ and $R_{\max} = 1$. Note that we choose these min and max values for simplicity, but because RL policies are invariant to positive scaling and affine translations [49], the actual numerical value of R_{\min} and R_{\max} can be chosen at the discretion of the user.

For Beam Rider we ran series of experiments for training the sophisticated reward DDT using a batch of $B = 10$ pairwise demonstrations where each demonstration is 25 states long and Adam optimizer, learning rate of 0.0009 with different seeds (see Appendix D for full details) and for analysing interpretability of the learned reward model on Beam Rider, we create a synthetic trace at each internal node. The synthetic trace creates a sequence of states with probability of routing left

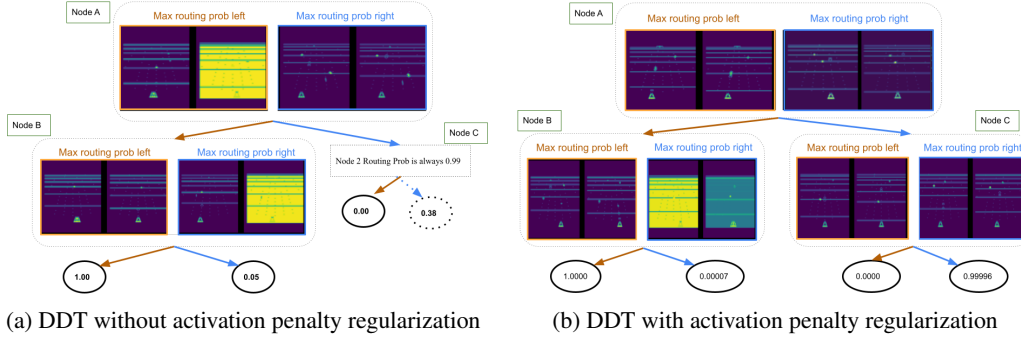


Figure 6: **Visualization of Beam Rider Reward DDTs.** We plot the DDTs trained without (a) vs with (b) a regularization penalty on the internal node routing probabilities. We find that the regularization helps the DDT use all leaf nodes, but hurts performance during RL (see Table 3)

Game	DDT				Baseline
	\neg penalty \neg argmax	\neg penalty argmax	penalty \neg argmax	penalty argmax	T-REX
Beam Rider	5212.04	725.84	793.12	3228.66	4742.68
Breakout	65.48	45.21	21.28	24.16	55.18

Table 3: **Reinforcement learning using reward DDTs.** We report performance averaged over 100 rollouts. We find that not using a regularization penalty (\neg penalty) and allowing a soft output (\neg argmax) achieves the best results, even performing slightly better than a large end-to-end neural network reward function (T-REX[15]).

monotonically decreasing. At an internal node, the trace begins with the state that has the maximum probability of being routed left and ends with the state that has the minimum probability of being routed left. For ease of visualization, we show the first and last state in the trace.

While trying to create the synthetic trace for internal nodes that are children of root node, we discovered that root node’s children nodes were using leaf nodes unequally, in the sense that one of child nodes of Node C was never used, subsequently the sub-tree that began at the unused node did not ever see any input state being routed to it. We re-trained the sophisticated reward DDT with the same hyperparameters, but with an added penalty regularization (see Appendix A) and after training, we re-created the synthetic traces for each internal node.

We similarly trained a reward DDT with and without penalty for Breakout as the DDT without penalty was unequally using its sub-trees(see Appendix E). And then on each of these learned reward functions, we optimized a policy by training a PPO agent for 50 million frames and compare it against the previous benchmark in learning from sub-optimal demonstrations, T-REX(Trajectory-ranked Reward EXtrapolation) [15]. T-REX’s architecture is similar to [18] and consists of 4 convolutional layers of sizes 7×7 , 5×5 , 3×3 and 3×3 with strides 3,2,1 and 1 respectively, where each convolutional layer has 16 filters and LeakyReLU as non-linearity, followed by a fully connected layer with 64 hidden units and a single scalar output.

For training the PPO agent, we utilize each learnt reward DDT in two ways: we either obtain a soft reward over all leaves from tree or we choose the path with maximum routing probability and the reward in this case is obtained by argmaxing over the maximum probability path.

Results We visualize the synthetic trace for each internal node in the sophisticated reward DDT trained without penalty Figure 6a and compare it against the synthetic traces of the sophisticated reward DDT trained using penalty Figure 6b. In (a) we see that Node A routes states where the agent hits an enemy ship to the left and states where it misses enemy ships to the right. Then Node B routes states where it looks like it will hit an enemy ship to a reward of 1.0 but interestingly routes states where it has hit an enemy ship to a reward of 0 (the yellow flash indicates an enemy being destroyed). This allows us to see a misalignment in the learned reward function. We investigated this further and found that when the agent loses a life, this also triggers a flashing yellow screen. Thus, the agent

appears to be misinterpreting the yellow flash and associating it with a penalty, when it should be associated with a reward. In Figure 6 (b) we see a similar trend for Node B.

In Table 3 we summarize the learned policy performance under 4 different scenarios: without Penalty without Argmax, without Penalty with Argmax, with Penalty without Argmax (returning the soft reward averaged over all leaf nodes), with Penalty with Argmax for both Beam Rider and Breakout in along with T-REX performance on each of these games. We see that RL performance is hurt by adding the regularization penalty. We achieve the best scores when using no penalty and a soft output. Interestingly, when using a regularization penalty, using a hard output of the DDT (returning the reward from the leaf node with highest probability) performs best.

5 Conclusion

We formulated and analyzed a novel method to learn an interpretable reward using differentiable decision trees. Our framework is capable of explaining the most significant features that determine the final reward and routing probability. In case of CartPole and GridWorld environments, our framework is capable of providing global explanations for all inputs. In case of Atari, we approximate global explanations by leveraging aggregations of local explanations by finding the input states that maximally and minimally activate the routing probability of each internal node.

On complex Atari reward learning benchmarks, we show that a shallow DDT can achieve better performance than a deep neural network reward function; however, this is only the case when we train a policy using soft outputs (path-probability-weighted average of all leaf nodes) from the reward DDT. If we instead train a policy only on the reward output from the most likely leaf node, then we find that there is a significant decrease in performance. These results provide a mixed message regarding the interpretability and viability of using reward DDTs. On the one hand, we provide evidence that reward DDTs are a viable alternative to end-to-end deep network rewards and can perform on-par and sometimes better than their deep neural network reward counterparts; however, for complex domains like Atari, this performance comes at the cost of using the DDT in a way that is not interpretable since using a soft output that is a weighted sum of the outputs of all leaf nodes makes the outputs of the reward DDT much harder to interpret. Ideally, we could use reward DDTs with hard reward outputs—the reward output during policy optimization would come from a single leaf node, allowing us to trace the reward output to a small number of binary routing decisions at the internal nodes. While this kind of hard output (argmax) process works well for the simpler domains we studied (e.g., CartPole and MNIST Gridworlds); it seems to hurt performance on more complex domains. We hypothesize this might be a result of the reward function being too sparse—the number of possible reward outputs is limited, which may adversely affect policy learning. Thus, our results reveal a tension between wanting highly shaped rewards to ensure good RL performance, while also wanting simple, non-shaped rewards to afford interpretability. Future work should investigate this trade-off in more depth.

Our experimental results also provide preliminary evidence that our framework can be used as an alignment debugger tool for inspecting learned reward functions for correctness and for capturing the features learned by a model that are mis-aligned with respect to human intent. An interesting area of future work in this direction entails using our framework to interpret existing pre-trained neural network reward models that are known to lead to unintended consequences [18, 32, 34, 60]. We hypothesize that reward DDTs could be useful in detecting the causes of mis-alignment and reward misidentification by distilling the pre-trained neural network reward models into reward DDTs. Once problems in a learned reward are identified, future work should also investigate how to fix a mis-aligned reward DDT by fine-tuning leaf and internal nodes based on human feedback. We hypothesize that recently proposed methods for human-in-the-loop representation and feature learning [10, 9] and methods for identifying causal features using small amounts of human annotations [25] could enable humans to easily and efficiently edit learned reward DDTs.

References

- [1] Ananye Agarwal, Ashish Kumar, Jitendra Malik, and Deepak Pathak. Legged locomotion in challenging terrains using egocentric vision. *CoRL*, 2022.

- [2] Rishabh Agarwal, Max Schwarzer, Pablo Samuel Castro, Aaron C Courville, and Marc Bellemare. Deep reinforcement learning at the edge of the statistical precipice. In M. Ranzato, A. Beygelzimer, Y. Dauphin, P.S. Liang, and J. Wortman Vaughan, editors, *Advances in Neural Information Processing Systems*, volume 34, pages 29304–29320. Curran Associates, Inc., 2021.
- [3] Saurabh Arora and Prashant Doshi. A survey of inverse reinforcement learning: Challenges, methods and progress. *Artificial Intelligence*, 297:103500, 2021.
- [4] M. G. Bellemare, Y. Naddaf, J. Veness, and M. Bowling. The arcade learning environment: An evaluation platform for general agents. *Journal of Artificial Intelligence Research*, 47:253–279, Jun 2013.
- [5] Marc G Bellemare, Yavar Naddaf, Joel Veness, and Michael Bowling. The arcade learning environment: An evaluation platform for general agents. *Journal of Artificial Intelligence Research*, 47:253–279, 2013.
- [6] Tom Bewley, Jonathan Lawry, Arthur Richards, Rachel Craddock, and Ian Henderson. Reward learning with trees: Methods and evaluation, 2023.
- [7] Tom Bewley and Freddy Lecue. Interpretable preference-based reinforcement learning with tree-structured reward functions. In *Proceedings of the 21st International Conference on Autonomous Agents and Multiagent Systems*, pages 118–126, 2022.
- [8] Erdem Biyik, Malayandi Palan, Nicholas C Landolfi, Dylan P Losey, Dorsa Sadigh, et al. Asking easy questions: A user-friendly approach to active reward learning. In *Conference on Robot Learning*, pages 1177–1190. PMLR, 2020.
- [9] Andreea Bobu, Yi Liu, Rohin Shah, Daniel S. Brown, and Anca D. Dragan. Sirl: Similarity-based implicit representation learning. In *Proceedings of the 2023 ACM/IEEE International Conference on Human-Robot Interaction (HRI)*, 2023.
- [10] Andreea Bobu, Marius Wiggert, Claire Tomlin, and Anca D Dragan. Inducing structure in reward learning by learning features. *The International Journal of Robotics Research*, 41(5):497–518, 2022.
- [11] Serena Booth, Sanjana Sharma, Sarah Chung, Julie Shah, and Elena L Glassman. Revisiting human-robot teaching and learning through the lens of human concept learning. In *2022 17th ACM/IEEE International Conference on Human-Robot Interaction (HRI)*, pages 147–156. IEEE, 2022.
- [12] Ralph Allan Bradley and Milton E Terry. Rank analysis of incomplete block designs: I. the method of paired comparisons. *Biometrika*, 39(3/4):324–345, 1952.
- [13] Greg Brockman, Vicki Cheung, Ludwig Pettersson, Jonas Schneider, John Schulman, Jie Tang, and Wojciech Zaremba. Openai gym. *arXiv preprint arXiv:1606.01540*, 2016.
- [14] Daniel S. Brown, Russell Coleman, Ravi Srinivasan, and Scott Niekum. Safe imitation learning via fast bayesian reward inference from preferences. In *International Conference on Machine Learning*, pages 1165–1177. PMLR, 2020.
- [15] Daniel S. Brown, Wonjoon Goo, Prabhat Nagarajan, and Scott Niekum. Extrapolating beyond suboptimal demonstrations via inverse reinforcement learning from observations. In *International conference on machine learning*, pages 783–792. PMLR, 2019.
- [16] Daniel S. Brown, Wonjoon Goo, and Scott Niekum. Better-than-demonstrator imitation learning via automatically-ranked demonstrations. In *Conference on robot learning*, pages 330–359. PMLR, 2020.
- [17] Daniel S. Brown, Jordan Schneider, Anca Dragan, and Scott Niekum. Value alignment verification. In *International Conference on Machine Learning*, pages 1105–1115. PMLR, 2021.
- [18] Paul F Christiano, Jan Leike, Tom B Brown, Miljan Martic, Shane Legg, and Dario Amodei. Deep reinforcement learning from human preferences. In *NIPS*, 2017.

- [19] Youri Coppens, Kyriakos Efthymiadis, Tom Lenaerts, Ann Nowé, Tim Miller, Rosina Weber, and Daniele Magazzeni. Distilling deep reinforcement learning policies in soft decision trees. In *Proceedings of the IJCAI 2019 workshop on explainable artificial intelligence*, pages 1–6, 2019.
- [20] Zihan Ding, Pablo Hernandez-Leal, Gavin Weiguang Ding, Changjian Li, and Ruitong Huang. Cdt: Cascading decision trees for explainable reinforcement learning, 2021.
- [21] Chelsea Finn, Sergey Levine, and Pieter Abbeel. Guided cost learning: Deep inverse optimal control via policy optimization. In *International conference on machine learning*, pages 49–58. PMLR, 2016.
- [22] Pedro Freire, Adam Gleave, Sam Toyer, and Stuart Russell. Derail: Diagnostic environments for reward and imitation learning. *arXiv preprint arXiv:2012.01365*, 2020.
- [23] Nicholas Frosst and Geoffrey Hinton. Distilling a neural network into a soft decision tree. *arXiv preprint arXiv:1711.09784*, 2017.
- [24] Gaurav R Ghosal, Matthew Zurek, Daniel S Brown, and Anca D Dragan. The effect of modeling human rationality level on learning rewards from multiple feedback types. *AAAI Conference on Artificial Intelligence*, 2023.
- [25] Gaurav Rohit Ghosal, Amrith Setlur, Daniel S. Brown, Anca Dragan, and Aditi Raghunathan. Contextual reliability: When different features matter in different contexts. In *International Conference on Machine Learning (ICML)*, 2023.
- [26] Leilani H Gilpin, David Bau, Ben Z Yuan, Ayesha Bajwa, Michael Specter, and Lalana Kagal. Explaining explanations: An overview of interpretability of machine learning. In *2018 IEEE 5th International Conference on data science and advanced analytics (DSAA)*, pages 80–89. IEEE, 2018.
- [27] Adam Gleave, Michael Dennis, Shane Legg, Stuart Russell, and Jan Leike. Quantifying differences in reward functions. In *International Conference on Learning Representations*, 2021.
- [28] Shixiang Gu, Ethan Holly, Timothy Lillicrap, and Sergey Levine. Deep reinforcement learning for robotic manipulation with asynchronous off-policy updates. In *2017 IEEE international conference on robotics and automation (ICRA)*, pages 3389–3396. IEEE, 2017.
- [29] Hussein Hazimeh, Natalia Ponomareva, Petros Mol, Zhenyu Tan, and Rahul Mazumder. The tree ensemble layer: Differentiability meets conditional computation. In *International Conference on Machine Learning*, pages 4138–4148. PMLR, 2020.
- [30] Alexandre Heuillet, Fabien Couthouis, and Natalia Díaz-Rodríguez. Explainability in deep reinforcement learning. *Knowledge-Based Systems*, 214:106685, 2021.
- [31] Zhewei Huang, Wen Heng, and Shuchang Zhou. Learning to paint with model-based deep reinforcement learning. In *Proceedings of the IEEE/CVF International Conference on Computer Vision*, pages 8709–8718, 2019.
- [32] Borja Ibarz, Jan Leike, Tobias Pohlen, Geoffrey Irving, Shane Legg, and Dario Amodei. Reward learning from human preferences and demonstrations in atari. *arXiv preprint arXiv:1811.06521*, 2018.
- [33] Donald Joseph Hejna III and Dorsa Sadigh. Few-shot preference learning for human-in-the-loop RL. In *6th Annual Conference on Robot Learning*, 2022.
- [34] Zaynah Javed*, Daniel S. Brown*, Satvik Sharma, Jerry Zhu, Ashwin Balakrishna, Marek Petrik, Anca D. Dragan, and Ken Goldberg. Policy gradient bayesian robust optimization. In *International Conference on Machine Learning (ICML)*, 2021.
- [35] Michael I Jordan and Robert A Jacobs. Hierarchical mixtures of experts and the em algorithm. *Neural computation*, 6(2):181–214, 1994.

- [36] Diederik P Kingma and Jimmy Ba. Adam: A method for stochastic optimization. *arXiv preprint arXiv:1412.6980*, 2014.
- [37] Sotiris B Kotsiantis. Decision trees: a recent overview. *Artificial Intelligence Review*, 39:261–283, 2013.
- [38] Victoria Krakovna, Jonathan Uesato, Vladimir Mikulik, Matthew Rahtz, Tom Everitt, Ramana Kumar, Zac Kenton, Jan Leike, and Shane Legg. Specification gaming: the flip side of ai ingenuity. *DeepMind Blog*, 2020.
- [39] Kimin Lee, Laura Smith, and Pieter Abbeel. Pebble: Feedback-efficient interactive reinforcement learning via relabeling experience and unsupervised pre-training. *arXiv preprint arXiv:2106.05091*, 2021.
- [40] Michael S Lee, Henny Admoni, and Reid Simmons. Machine teaching for human inverse reinforcement learning. *Frontiers in Robotics and AI*, 8:693050, 2021.
- [41] Jan Leike, David Krueger, Tom Everitt, Miljan Martic, Vishal Maini, and Shane Legg. Scalable agent alignment via reward modeling: a research direction. *arXiv preprint arXiv:1811.07871*, 2018.
- [42] Yi Liu, Gaurav Datta, Ellen Novoseller, and Daniel S Brown. Efficient preference-based reinforcement learning using learned dynamics models. In *2023 IEEE International Conference on Robotics and Automation (ICRA)*. IEEE, 2023.
- [43] Shaunak A Mehta and Dylan P Losey. Unified learning from demonstrations, corrections, and preferences during physical human-robot interaction. *arXiv preprint arXiv:2207.03395*, 2022.
- [44] Eric J Michaud, Adam Gleave, and Stuart Russell. Understanding learned reward functions. *arXiv preprint arXiv:2012.05862*, 2020.
- [45] Volodymyr Mnih, Koray Kavukcuoglu, David Silver, Alex Graves, Ioannis Antonoglou, Daan Wierstra, and Martin Riedmiller. Playing atari with deep reinforcement learning. *arXiv preprint arXiv:1312.5602*, 2013.
- [46] Christoph Molnar. *Interpretable machine learning*. Lulu. com, 2020.
- [47] Andrew Y Ng, Daishi Harada, and Stuart Russell. Policy invariance under reward transformations: Theory and application to reward shaping. In *Icml*, volume 99, pages 278–287, 1999.
- [48] Alizée Pace, Alex J. Chan, and Mihaela van der Schaar. Poetree: Interpretable policy learning with adaptive decision trees, 2022.
- [49] Martin L. Puterman. *Markov Decision Processes: Discrete Stochastic Dynamic Programming*. John Wiley & Sons, Inc., USA, 1st edition, 1994.
- [50] Tilman Räuukur, Anson Ho, Stephen Casper, and Dylan Hadfield-Menell. Toward transparent ai: A survey on interpreting the inner structures of deep neural networks. *arXiv preprint arXiv:2207.13243*, 2022.
- [51] Stuart Russell, Daniel Dewey, and Max Tegmark. Research priorities for robust and beneficial artificial intelligence. *Ai Magazine*, 36(4):105–114, 2015.
- [52] Dorsa Sadigh, Anca D Dragan, Shankar Sastry, and Sanjit A Seshia. Active preference-based learning of reward functions. In *Robotics Science and Systems*, 2017.
- [53] Dorsa Sadigh, Anca D Dragan, Shankar Sastry, and Sanjit A Seshia. Active preference-based learning of reward functions. In *Robotics: Science and Systems*, 2017.
- [54] Lindsay Sanneman and Julie A. Shah. An empirical study of reward explanations with human-robot interaction applications. *IEEE Robotics and Automation Letters*, 7(4):8956–8963, 2022.
- [55] John Schulman, Filip Wolski, Prafulla Dhariwal, Alec Radford, and Oleg Klimov. Proximal policy optimization algorithms. *arXiv preprint arXiv:1707.06347*, 2017.

- [56] Daniel Shin, Anca Dragan, and Daniel S. Brown. Benchmarks and algorithms for offline preference-based reward learning. *Transactions on Machine Learning Research*.
- [57] Andrew Silva, Matthew Gombolay, Taylor Killian, Ivan Jimenez, and Sung-Hyun Son. Optimization methods for interpretable differentiable decision trees applied to reinforcement learning. In *International conference on artificial intelligence and statistics*, pages 1855–1865. PMLR, 2020.
- [58] Pradyumna Tambwekar, Andrew Silva, Nakul Gopalan, and Matthew Gombolay. Natural language specification of reinforcement learning policies through differentiable decision trees. *IEEE Robotics and Automation Letters*, pages 1–8, 2023.
- [59] Ryutaro Tanno, Kai Arulkumaran, Daniel Alexander, Antonio Criminisi, and Aditya Nori. Adaptive neural trees. In *International Conference on Machine Learning*, pages 6166–6175. PMLR, 2019.
- [60] Jeremy Tien, Jerry Zhi-Yang He, Zackory Erickson, Anca Dragan, and Daniel S Brown. Causal confusion and reward misidentification in preference-based reward learning. In *International Conference on Learning Representations*, 2023.
- [61] Christian Wirth, Riad Akrou, Gerhard Neumann, Johannes Fürnkranz, et al. A survey of preference-based reinforcement learning methods. *Journal of Machine Learning Research*, 18(136):1–46, 2017.
- [62] Christian Wirth, Johannes Fürnkranz, and Gerhard Neumann. Model-free preference-based reinforcement learning. In *Thirtieth AAAI Conference on Artificial Intelligence*, 2016.
- [63] Ruihan Yang, Minghao Zhang, Nicklas Hansen, Huazhe Xu, and Xiaolong Wang. Learning vision-guided quadrupedal locomotion end-to-end with cross-modal transformers. In *International Conference on Learning Representations*, 2022.
- [64] Valentina Zantedeschi, Matt J Kusner, and Vlad Niculae. Learning binary trees by argmin differentiation. *ICML*, 2021.
- [65] Quan-shi Zhang and Song-Chun Zhu. Visual interpretability for deep learning: a survey. *Frontiers of Information Technology & Electronic Engineering*, 19(1):27–39, 2018.
- [66] Zhejun Zhang, Alexander Liniger, Dengxin Dai, Fisher Yu, and Luc Van Gool. End-to-end urban driving by imitating a reinforcement learning coach. In *Proceedings of the IEEE/CVF international conference on computer vision*, pages 15222–15232, 2021.

A DDT Routing Penalty Regularization

We take inspiration from [19] for adding penalty regularization and we first explain how penalty is defined at each internal node and then elaborate on calculating penalty for a single state over the whole DDT.

The cross-entropy between desired routing probability distribution of an internal node such that it’s children nodes are equally used and the actual routing probability distribution is referred to as Penalty and is given by

$$\alpha_i = \frac{\sum_{\mathbf{x}} P^i(\mathbf{x}) p_i(\mathbf{x})}{\sum_{\mathbf{x}} P^i(\mathbf{x})} \quad (9)$$

where the probability of a current internal node is $p_i(\mathbf{x})$ and path probability from root node to an internal node is $P^i(\mathbf{x})$.

Penalty over the whole DDT for a single state is defined as sum over all internal nodes for the given input \mathbf{x}

$$C = -\lambda \sum_{i \in \text{Inner Nodes}} 0.5 \log(\alpha_i) + 0.5 \log(1 - \alpha_i) \quad (10)$$

where hyper-parameter λ controls the strength of penalty λ in reward DDT so that the penalty strength is proportional to 2^{-d} and decays exponentially with depth of tree. Finally the penalty term for learning reward tree from pairwise preferences is calculated by taking the mean over all penalties for all states in the pairwise demonstrations.

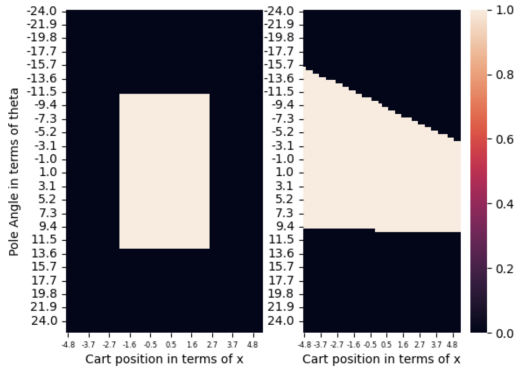


Figure 7: **Cartpole Reward DDT**. Ground Truth Reward on the left compared to Learnt Reward on the right. The reward model learnt by DDT is missing vertical boundaries visually, implying that it failed to pick up on cart position when contrasted with ground truth reward model that has both horizontal and vertical boundaries corresponding to pole angle and cart position respectively.

B Additional Cartpole Analysis

To verify that our DDT reward model picks up on the misalignment in the reward function with respect to input features, particular cart position, we also compared the ground truth reward with the output of the learned reward obtained by taking the argmax class from the leaf node with maximum routing probability. We plot these two rewards as a function of pole angle and cart position in Figure 7

Figure 7 depicts that the learned reward is misaligned: the reward DDT has learned to approximate the preferences over pole angle, but pays much less attention to the pole angle when predicting rewards.

C MNIST (0-3) Gridworld Additional Results and Analysis

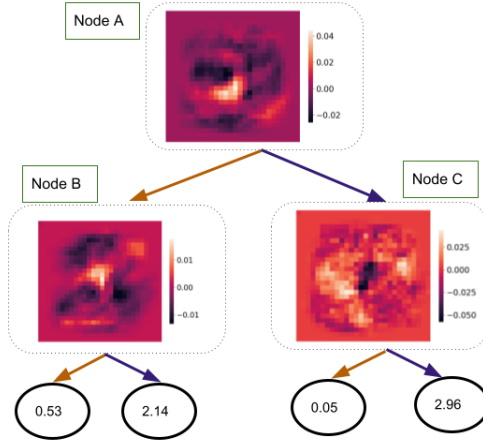
In this section we provide detailed analysis about interpretability of different DDTs, beginning from comparison between Reward DDT and Classification DDT, then comparing Reward DDTs constructed using two different leaf node formulations, followed by comparison of different regularization on a reward DDT.

C.1 Min-Max Reward Interpolation Tree vs Classification tree

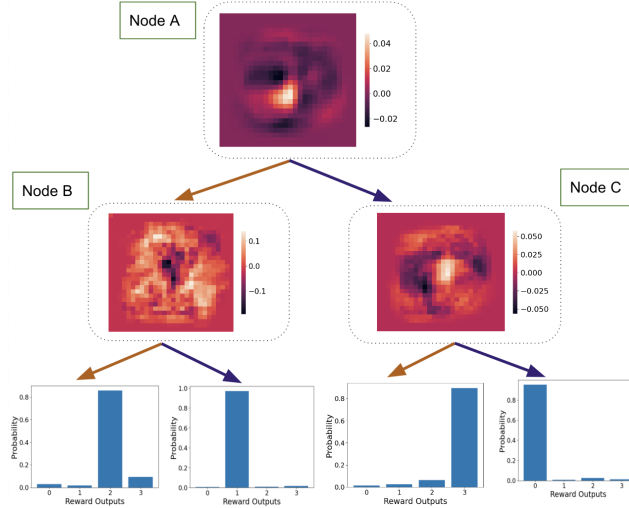
We train a DDT with explicit reward labels and a classification loss, as in, we re-produce the classification DDT from [19] and compare it to reward tree learned using preferences (refer to Sec 4.2.2 of main paper).

For comparison of reward tree against the classification tree trained using ground truth labels, we plot the heatmaps of internal nodes in both the trees and our results in Figure 8 give evidence that reward tree can capture visual features without any loss in interpretability when compared to the one learnt from simple ground truth labels, even though preferences used here are weaker supervision than ground truth labels since preferences used in our experiments are binary as compared to ground truth labels which are 0,1,2,3 corresponding to each actual digit image. This is particularly important in cases where explicit labels are either missing or are hard to be specified or require intensive user-input efforts.

In Figure 8b Node A activates strongly for pixels in the middle of 1s and 2s, routing them left, while 0s and 3s are routed right. Node B routes left for vertical pixels in the center and sends 2's



(a) Reward Tree trained using preferences



(b) Classification Tree trained on ground truth label

Figure 8: Visualization of MNSIT (0-3) Reward vs Classification Tree

left and 1's right (note the light shadow looks like a 2 while the darker shadow in the middle that looks like a 1). Node C learns to distinguish between 0s and 3s, routing 3s left and 0s right. This is comparable to the activation heatmaps of the node probability distribution at each of the internal node described for reward tree (in Sec 4.2.2 of main paper).

C.2 Min-Max Reward Interpolation Leaf DDT vs Multi-Class Reward Leaf DDT

We train and compare two reward DDTs with simple internal node architecture but with different leaf formulations using the same Bradley-Terry loss over preference demonstration in Figure 9 by visualizing the activation heatmaps of routing probability distributions for the internal nodes and the leaf distribution for each leaf node.

In Figure 9b, each internal node learns to capture almost the same visual feature while the leaf nodes fail to specialize as the argmax output from first two leaf nodes is always a 0 and last two leaf nodes always return a 3. Multi-class Leaf DDT fails to pick up on individual digit in the trajectory, despite requiring the user to input discrete reward vector whereas in the Min-Max Interpolation Leaf DDT each internal node captures different visual attributes and each of the leaf nodes in the interpolated reward DDT is specialized, even though no discrete reward values were given as an input.

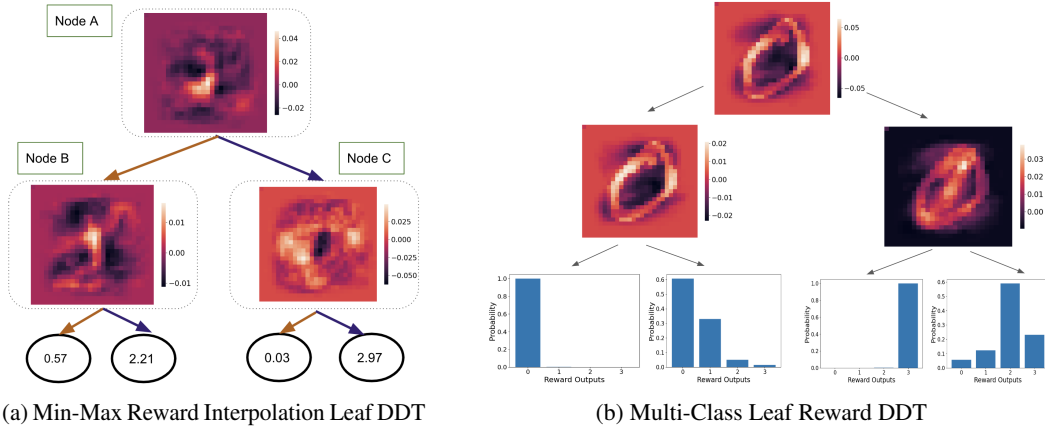


Figure 9: Visualization of MNSIT (0-3) Reward Trees: Min-Max Reward Interpolation Leaf vs Multi-Class Leaf

This shows that Min-Max Reward Interpolation Leaf DDT is beneficial over Multi-Class Reward Leaf DDT with respect to interpretability and also in terms of human-input efforts. for all states in the pairwise demonstrations.

C.3 Min-Max Reward Interpolation DDTs with Simple Internal Nodes vs Sophisticated Internal Node

We compare our 2 methods of constructing internal nodes for a reward DDTs.

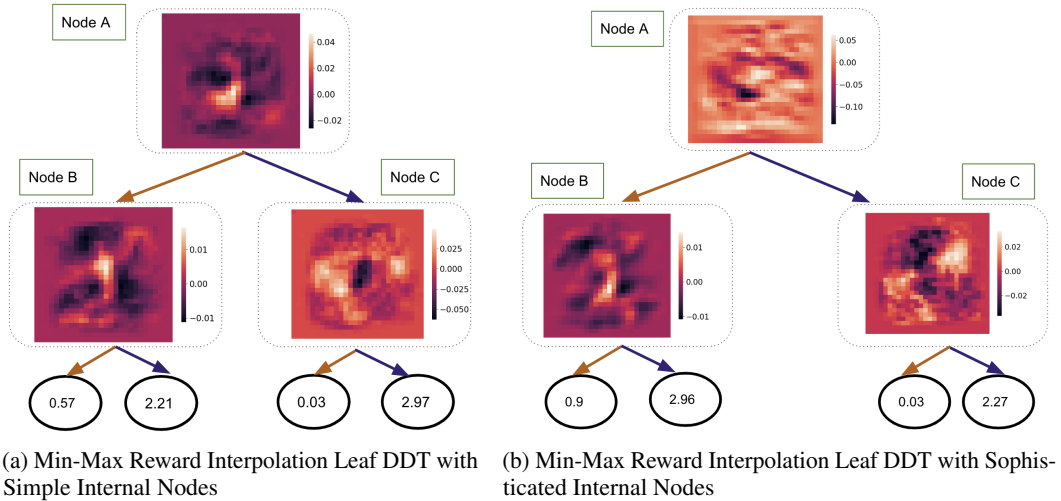


Figure 10: Visualization of MNSIT (0-3) Reward Trees :Simple Internal Node vs Sophisticated Internal Node

Since Min-Max Reward Interpolation Leaf DDT outperforms Multi-Class Reward Leaf DDT, hence we train two different Min-Max Reward Interpolation Leaf DDTs, first one with simple internal nodes and second one with sophisticated internal nodes where a sophisticated internal node contains a single convolutional layer with filter of size 3x3 and stride 1 with Leaky ReLU as the non-linearity followed by the fully connected layer.

In Figure 10b Node A activates strongly for pixels in the middle of 1s and 3s, routing them left, while 0s and 3s are routed right. Node B routes left for vertical pixels in the center and sends 1's left and 3's right (note the darker shadow in the middle that looks like a 3). Node C learns to distinguish between 0s and 2s, routing 0s left and 2s right. This is comparable to the activation heatmaps of the

node probability distribution at each of the internal node described for reward tree(in Sec 4.2.2 of main paper).

Our results depict that in a medium-complexity environment with visual inputs , both DDTs yield relatively equal interpretability but with a higher-complexity environment with larger visual input size such as Atari, the reward DDT with sophisticated node should be used as convolution layer with non-linearity are more powerful in terms of processing an input than a simple fully connected layer.

C.4 Multi-Class Reward Leaf DDT Regularization

Since the DDT with Multi-Class Reward Leaves failed to specialize, this lead us to add the penalty term to the Bradley-Terry preference loss for training the Multi-Class Reward Leaf DDT.

For training the Reward DDT,we calculate penalty over batch of 50 pairwise demonstrations where each demonstration contains a single 28x28 greyscale image.To check interpretability, we plot the activation heatmaps of routing probability distributions for the internal nodes and the leaf distribution for each leaf node in Figure 11a and the resulting plots are hugely pixelated, causing a loss in interpretability.

Following this, we increase the temporal window size for calculating penalty, as suggested in [19], and thus we calculate penalty over a pair of 50 preference demonstration where each demonstration is now 50 states long, as opposed to previous case where each demonstration contained a single state. And we again visualize the heatmaps at internal nodes and leaf distributions for each leaf node in Figure 11b. The heatmaps here are little better in contrast to Figure 11a but still have a huge loss of interpretability as compared to Figure 9b.

D Atari: Beam Rider

For training Min-Max Reward Interpolation Leaf DDT with sophisticated internal nodes on Beam Rider we tried all combinations possible using the following hyper-parameter settings:

- Seed : 0, 1 and 2
- Batch size of Pairwise Preferences B : 1,10
- Learning Rate: 0.00005, 0.0009 for B equal to 1 and 10 respectively

But for all DDTs trained without the penalty, we ran into the problem of un-equal use of sub-trees.For running-RL and visualizing the synthetic traces we use the reward DDT, trained using seed 0 with $B=10$ and $lr=0.0009$.

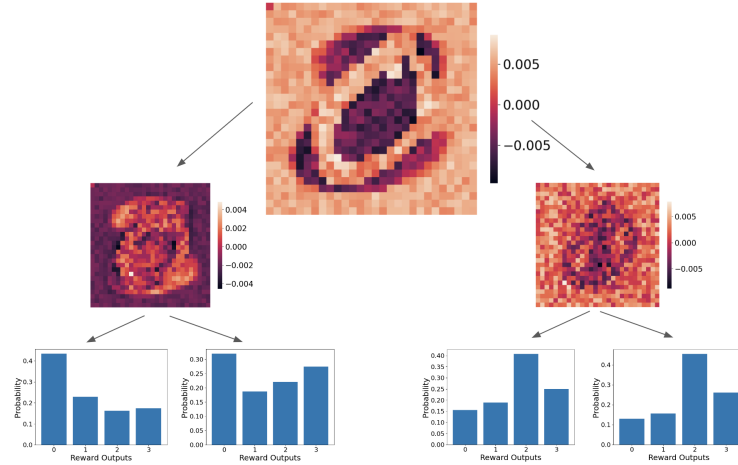
Note: we use the same exact setting for training the reward DDT with penalty.

E Atari:Breakout

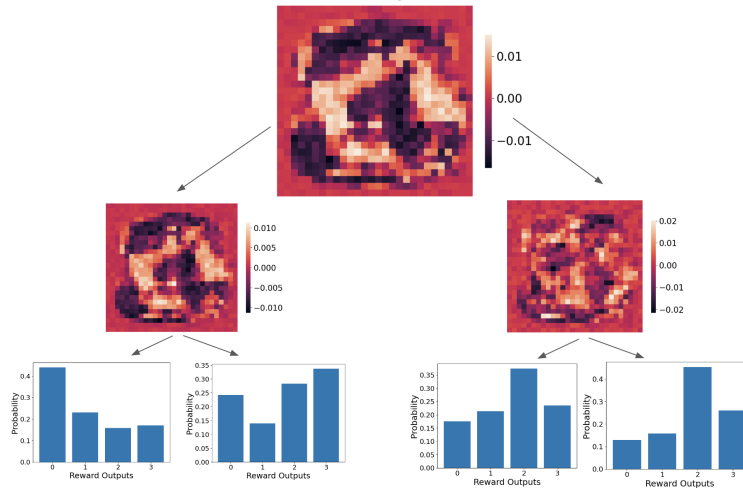
We trained 2 different Interpolated Leaf DDTs on Breakout, one without and another with Penalty added and created the synthetic trace over all input states starting from states that are routed 100% to left and ending at states that are routed complete right (as in have 0% probability of being routed left).

For Breakout , we show a more rigorous trace than BeamRider,by visualizing states that are routed with 100% , 75% , 50% , 25% and 0% probability to left. And we found that, fig 12 without any penalty added both children nodes of the root node only use their respective left leaves and do not route any state to their respective right leaves. This meant that a synthetic trace could not be visualized for either Node B or Node C.

Next, we visualize the synthetic trace over the penalized DDT, fig 13 and surprisingly , we found that the regularization term added to the final loss of the tree while training was penalizing the DDT so heavily that now the routing probability at Node B and Node C was always between 0.5 and 0.499, which again lead to a failure in being able to create the synthetic trace over inputs as no states were now being routed with a 100% probability neither left nor right and also numerically the difference in routing probability was very trivial.



(a) Multi-Class Leaf Reward DDT with penalty calculated over a batch of 50 pairwise preference demonstrations where each demonstration has a single state



(b) Multi-Class Leaf Reward DDT with penalty calculated over a batch of 50 pairwise preference demonstrations where each demonstration has a single state

Figure 11: Multi-Class Leaf Reward DDT with penalty calculated over different temporal window lengths

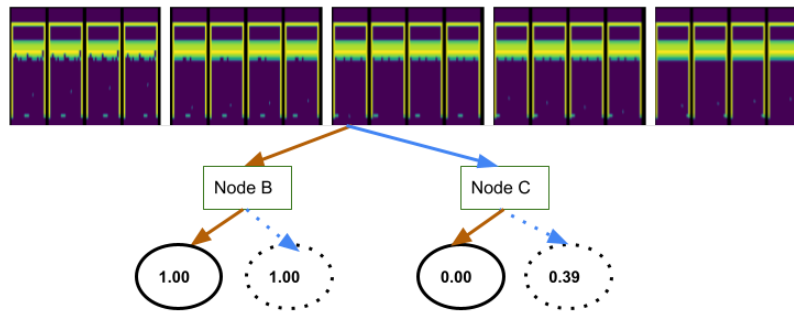


Figure 12: Interpolated DDT of depth 1 trained on Breakout without regularization

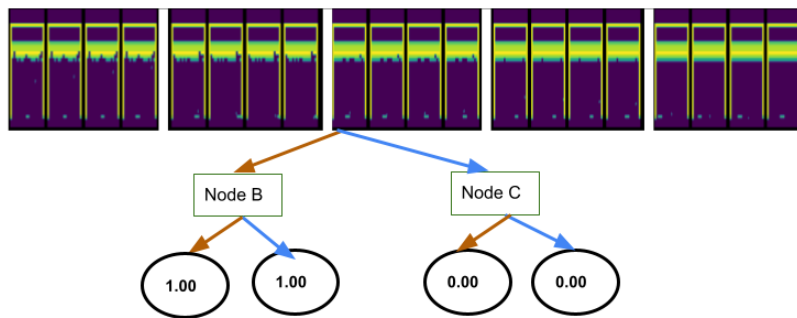


Figure 13: Interpolated DDT of depth 1 trained on Breakout with regularization